Hydrogels Hot Paper

Deutsche Ausgabe: DOI: 10.1002/ange.201409134
Internationale Ausgabe: DOI: 10.1002/anie.201409134

Control of Stem-Cell Behavior by Fine Tuning the Supramolecular Assemblies of Low-Molecular-Weight Gelators**

*Laurent Latxague, Michael A. Ramin, Ananda Appavoo, Pierre Berto, Mathieu Maisani, Camille Ehret, Olivier Chassande, and Philippe Barthélémy**

Abstract: *Controlling the behavior of stem cells through the supramolecular architecture of the extracellular matrix remains an important challenge in the culture of stem cells. Herein, we report on a new generation of low-molecular-weight gelators (LMWG) for the culture of isolated stem cells. The bola-amphiphile structures derived from nucleolipids feature unique rheological and biological properties suitable for tissue engineering applications. The bola-amphiphile-based hydrogel scaffold exhibits the following essential properties: it is nontoxic, easy to handle, injectable, and features a biocompatible rheology. The reported glycosyl-nucleoside bola-amphiphiles (GNBA) are the first examples of LMWG that allow the culture of isolated stem cells in a gel matrix. The results (TEM observations and rheology) suggest that the supramolecular organizations of the matrix play a role in the behavior of stem cells in 3D environments.*

The development of biocompatible artificial matrixes that can be used for the culture of stem cell remains a great challenge in tissue engineering and/or regenerative medicine.[1–5] Recent studies in these promising fields have focused on understanding the physicochemical parameters that control the fate of stem cells.[6,7] While several studies have concentrated on the impact of biochemical cues on the behavior of stem cells, it has been demonstrated that the mechanical properties of the microenvironment play a major role on a wide variety of cells including stem cells.[8] The matrix stiffness is known to affect the behavior of cardiac cells,[9] glial cells[10] and mesenchymal stem cells.[11,12] Most of these studies used gel scaffolds based on polymeric materials that were derived from either natural sources or chemical synthesis. However, polymers often suffer from several limitations, including poor biocompatibility, toxicity, biodegradability, proinflammatory activity etc. Alternatively, small-molecule-based hydrogels, involving low-molecular-weight gelators (LMWG), are emerging as a promising tool for regenerative medicine strategy capable of restoring biological and mechanical properties and/or function.[13]

Bola-amphiphiles are composed of one or two hydrophobic chains that are covalently linked at both ends to hydrophilic head groups.[14] This type of molecular architecture can be found in archaebacteria membranes,[15] and has been used in numerous applications, ranging from nanomaterial synthesis to drug or gene delivery.[16] The advantage of using nucleosides in a bola-amphiphile design was first described by Shimizu in 2002.[17] We hypothesized that bola-amphiphile architectures could lead to LMWG-based hydrogels suitable for the culture of stem cells and tissue-engineering applications.

Here, we report the first use of bola-amphiphile-based hydrogels in the adhesion and proliferation of stem cells. Contrary to the previously reported glycosyl-nucleoside lipids (GNL)[18] and glycosyl-nucleoside fluorinated amphiphile (GNF),[13] which suffer from biological and rheological limitations, the glycosyl-nucleoside bola-amphiphiles (GNBA) offer a new biocompatible microenvironment for the culture of stem cells. GNBA-based gels feature improved mechanical properties, including a stiffness that allows a process called mechanotransduction,[19] which is required for tissue-engineering applications (Figure 1).

The synthesis of GNBAs **1**, **2**, and **3** (depicted in Scheme 1) relies mainly on a double click-chemistry strategy as used in most of our earlier works (see the Supporting Information for details). For compounds **1** and **2**, gel formation was observed in water at 1% (w/v). On the other hand, bola-amphiphile **3** was unable to stabilize a gel, indicating that nucleoside moiety is required for gel stabilization. Transmission electron microscopy (TEM) images of the hydrogel obtained from GNBA **1** show the formation of an anisotropic fibrillar network. This network is densely interconnected through straight fibers of 6–9 nm in width (see the Supporting Information, Figure S3A), which likely contribute to the high storage modulus that can be observed. Note that under similar conditions, dissymmetric bola-amphiphile **2** and GNF exhibit bundles of nanofibers with fewer connections (see the Supporting Information, Figure S3B and Figure S3C).

To further understand the molecular organization and packing profile within the supramolecular structures, small-angle X-ray scattering (SAXS) experiments were performed at room temperature. The small-angle diffraction patterns of

[*] Dr. L. Latxague, Dr. M. A. Ramin, A. Appavoo, P. Berto, Prof. P. Barthélémy
Univ. Bordeaux, ARNA laboratory, F-33000 Bordeaux (France)
E-mail: philippe.barthelemy@inserm.fr
M. Maisani, C. Ehret, Dr. O. Chassande
INSERM, U1026, BIOTIS laboratory, F-33000 Bordeaux (France)

[**] The authors acknowledge financial support from the French National Agency (ANR) in the frame of its program Blanc "GelCells" SIMI 7-2010 and the Conseil Régional d'Aquitaine (CRAq). We acknowledge the Army Research Office for financial support. The authors would like to thank Andrew Goldsborough and Brice Kauffmann for proof-reading the MS and SAXS experiments, respectively.

Supporting information for this article (including experimental procedures and characterization data, such as NMR, MS, and DLS results, and TEM images) is available on the WWW under http://dx.doi.org/10.1002/anie.201409134.

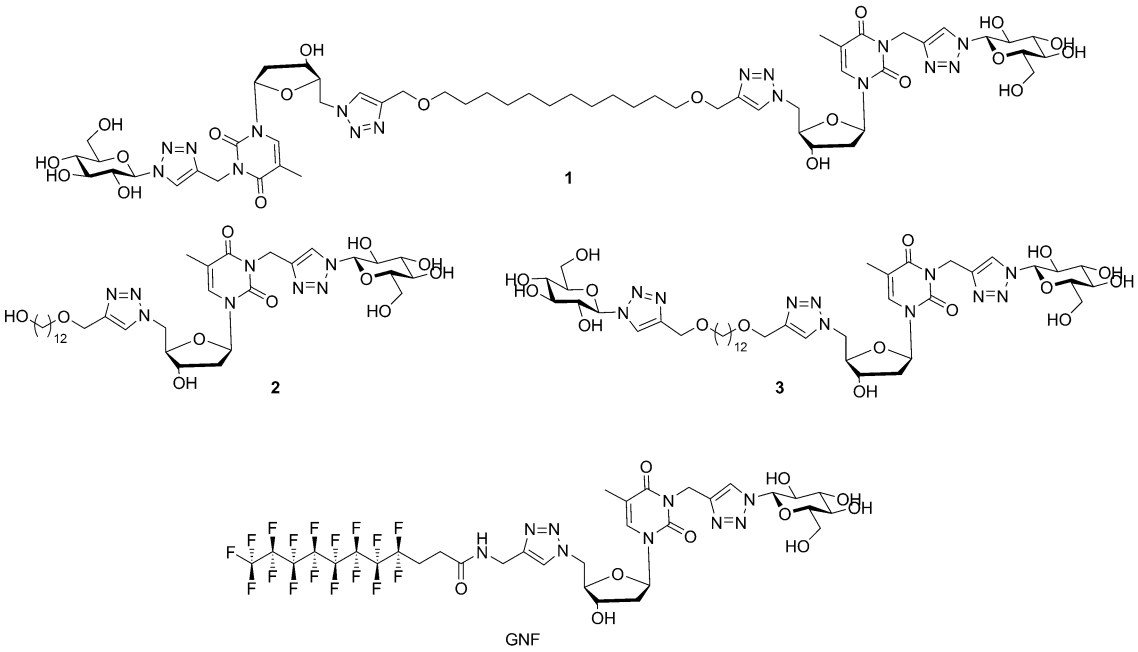

Scheme 1. Structures of bola-amphiphiles synthesized for this study, compared with glycosyl-nucleoside fluorinated amphiphile (GNF).

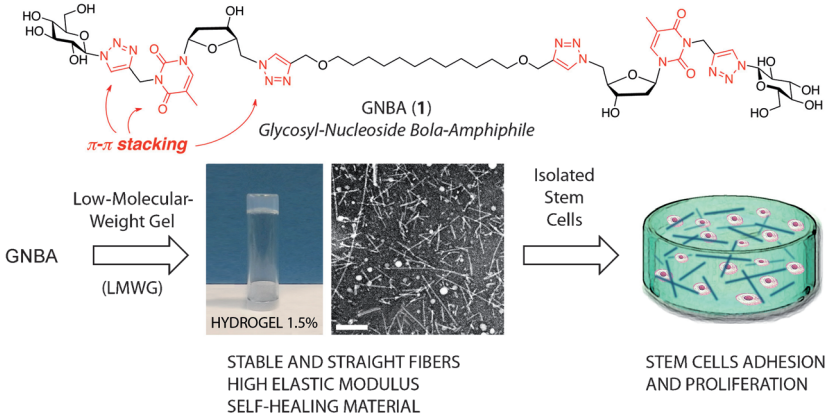

Figure 1. Formation of the LMWG scaffold suitable for the culture of stem cells. GNBA self-assemble through six π–π interactions per molecule to provide stable and straight fibers. The resulting self-healing hydrogels feature stiffness properties, which allow the adhesion and proliferation of stem cells. Scale bar: 200 nm.

aqueous samples (GNBA **1** at 30%, w/v) show a diffraction peak at 3.1 nm (see the Supporting Information, Figure S4). This repeat period, which corresponds roughly to the molecular length of GNBA **1** (4 nm in extended conformation, calculated by MM+ force field modeling), suggests that two molecules are tightly associated in the thin fibers.

The molecular scaffold of the gel is formed through noncovalent interactions, such as hydrogen bonds, π–π stacking interactions, van der Waals interactions etc.[20] Interestingly, GNBAs contain, among other groups, a 1,2,3-triazole ring and a nucleoside, which can be involved in the formation of supramolecular assemblies.[21] To highlight their role in the self-assembly process, an NMR study was realized by adding water to a solution of bola-amphiphiles **1** and **2** in [D_6]DMSO (Figure 2). The addition of water to the sample led to an upfield shift of the triazole hydrogen atom and the thymidine hydrogen atom H-5′, which indicates the contribution of both triazole and nucleobase π–π stacking to the aggregation phenomenon. The temperature-dependent ^{1}H NMR study also confirms the presence of π–π stacking interactions between the aromatic moieties. In this case, these signals are deshielded with the increase in temperature (see the Supporting Information, Figure S2).

The mechanical behavior of our hydrogels was estimated by rheology. All rheological experiments were conducted within the linear viscoelastic region. We studied the variation of storage modulus (G′) and loss modulus (G″) as a function of the applied frequency. The storage modulus (G′), also called the elastic modulus, describes the amount of the energy that is stored and released in each oscillation. The loss modulus (G″), also called the viscous modulus, corresponds to the energy dissipated as heat (and therefore lost). For all our hydrogels, the storage modulus exceeded that of the loss modulus and their values were weakly dependent on the frequency in the entire range that we tested, which indicates the formation of a stable gel (Figure 3).

In order to evaluate the relative strength of the hydrogels, we compared the storage moduli at an angular frequency of 1 rad s^{-1}. The G′ value for hydrogel **1** (30325 Pa) is much higher than the value obtained for the GNF hydrogel (1749 Pa) at the same concentration (11.55 mM). This observation suggests the formation of a more rigid and "solid-like"

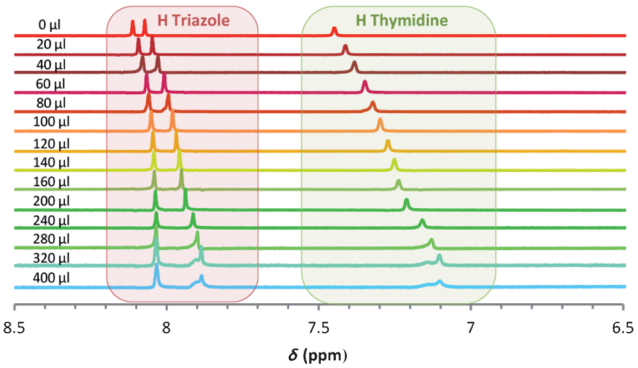

Figure 2. Partial ^{1}H NMR spectra of GNBA (compound **1**) showing the resonance signals of triazole and H5′-thymidine hydrogen atoms. Spectra were recorded in [D$_6$]DMSO (7 mg of compound **1** in 0.5 mL [D$_6$]DMSO) with increasing amounts of water.

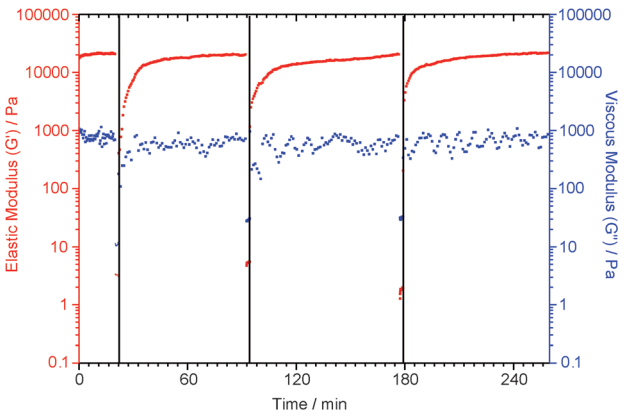

Figure 4. Step–strain measurement of the hydrogel **1** at 1 % (w/v) at a fixed angular frequency of 6.283 rad/s. The gel was successively swept from 0.03 % to 15 % strain, then back to 0.03 % strain.

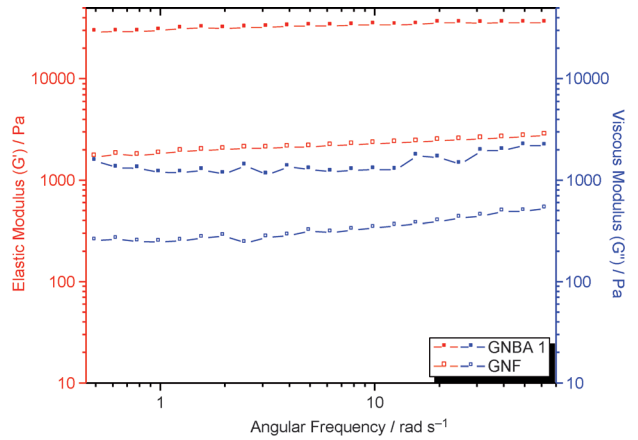

Figure 3. Frequency sweep results for hydrogels obtained from compound **1** and GNF (at 11.55 mM) at a constant strain of 0.03 %.

material with the hydrogel obtained from the symmetrical bola-amphiphile. The elastic character is significantly improved with the GNBA **1** compared to the GNF analogue. However, the elastic modulus is much lower with the unsymmetrical bola-amphiphile **2** (see the Supporting Information, Figure S6) at the same concentration (23.10 mM). This result may be explained by fewer interactions between the nucleoside and triazole moieties of compound **2** (three π–π stacking interactions instead of six for GNBA **1**).

For some biomedical applications, a hydrogel should be delivered by syringe, thereby preventing the pain of a surgical implantation.[22] Therefore, this injectable hydrogel must regain its strength after the injection (the withdrawal of external stress). The gel obtained from compound **1** can be shaken vigorously by hand and the sample immediately recovers its gel behavior. This thixotropic property was studied in more detail by rheology. The experiment consists in applying a high strain to the sample and studying the evolution of the viscoelastic moduli (Figure 4). First, a low strain of 0.03 % was applied to gel **1** at 1 % (w/v) for 20 min. In the gel state, G′ was larger than G″. Then, gel **1** was suddenly subjected to a higher strain of 15 % for 2 min. At this point, the G′ value was much lower indicating the collapse of the gel, that is, the gel liquefies under the stress. With a strain of 0.03 % (as in the first step), the sample gradually returns to the gel state and recovers its original strength. Indeed, the G′ value increases rapidly and the sample recovers approximately 80 % of its initial elastic modulus within 15 min. This experiment was repeated at least three times to verify its reproducibility (see the Supporting Information, Figure S7). The therapeutic applicability of the thixotropic behavior of GNBA-based gel was challenged in a mouse model using subcutaneous injection. The GNBA solution was drawn into a syringe and left at room temperature until gelation. Then the gel was pushed with the piston through a 16-gauge needle, resulting in a gel–sol transition that allowed the injection of the solution under the skin of an anaesthetized mouse (see movie, see the Supporting Information). 2 h after injection, a superficial examination of the tissue after skin biopsy showed the presence of a bulk of gel that displayed an ovoid shape and was easily distinguishable from the surrounding fat tissue. Sections showed the gel structure as small fibers that did not contain any cells or matrix surrounded by host tissue (see the Supporting Information, Figure S11). This experiment emphasizes the injectability of the GNBA gel by taking advantage of its thixotropic property.

In order to evaluate the biocompatibility of the GNBA **1**, we carried out cytotoxicity and cytocompatibility studies. For this purpose, human mesenchymal stem cells isolated from adipose tissue (ASC) were grown for four days in the presence of GNBA at increasing concentrations. The toxicity was evaluated by a MTT test (colorimetric assay for assessing cell viability using a tetrazolium dye). No toxicity was found for concentrations up to 50 µM (see Supporting Information, Figure S8).

In order to evaluate the behavior of cells in the LMWG matrixes, different cell types were embedded in the GNBA gel (3 % GNBA, w/v). The GNBA gels were initially prepared without cells and heated at 55 °C for 30 min to obtain a liquid phase. After cooling to 37 °C, the cells were mixed with the GNBA solution and the mixture was incubated at 25 °C under gentle stirring.

The rat preosteoblastic cell line D1 was first grown within the gel. The cell concentration was longitudinally followed using a nontoxic metabolic activity assay with alamar blue. This analysis showed a moderate increase of the number of cells over two weeks. The same experiment was performed with human ASCs, showing a stability of the number of cells, with a slight decrease two weeks after seeding (see the Supporting Information, Figure S9). Altogether these data show that neither low concentrations of soluble GNBA nor high GNBA concentrations, which could result in gel formation, have toxic effects on cells.

The human ASCs cells embedded in the gels were examined by confocal microscopy and submitted to a live–dead assay to assess the cell viability. In the case of GNBA **1**, 24 h after seeding, all cells were attached to the gel scaffold and were viable (Figure 5). Most of the cells appeared round,

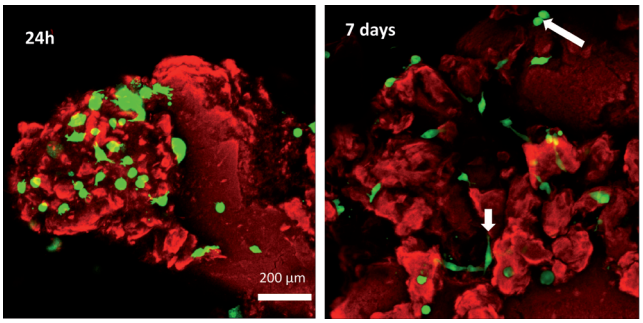

Figure 5. Pictures of GNBA-gel-embedded human ASCs grown for 24 h or 7 days (obtained by stacking of 10 images, representing 100 µm thickness in the *z* axis). The top white arrow points to a dividing cell. The bottom white arrow points to a fibroblastoid cell. Cells are stained green (calcein), wheras the GNBA gel is stained red, as it incorporates the ethidium molecule. Scale bar: 200 µm.

however, some cells exhibited a fibroblastoid phenotype, typical of cell adhesion. One week after seeding, the cells had scattered within the gel and most of them showed a fibroblastoid morphology. A vast majority of green (living) cells was found. Cell divisions were occasionally observed, too. In contrast, in the case of the GNF hydrogel, which exhibited weak stiffness properties ($G' = 1.7$ kPa), isolated cells showed a round morphology and failed to survive over four days (see the Supporting Information, Figure S10). As GNBA **1** and GNF share the hydrophilic moieties glucose and thymidine, the more favorable behavior of stem cells in GNBA gels can be attributed to the 3D organization of the scaffold. This is characterized by a higher mechanical resistance (GNBA, $G' =$ 30 kPa), which promotes cell adhesion and spreading.[23]

In summary, we have developed a scalable synthesis of self-healing hydrogels using glycosyl-nucleoside bola-amphiphiles as low-molecular-weight gelators (LMWG). These biocompatible hydrogels feature a high elastic modulus, which allows the adhesion and the proliferation of isolated stem cells. To our knowledge, this is the first time that the influence of the modulus of LMWGs on the fate of stem cells was demonstrated. Three-dimensional scaffolds based on biocompatible LMWGs that control the fate of stem cells would be very useful for applications in regenerative medicine and tissue engineering.

Keywords: amphiphiles · hydrogels · stem cells · supramolecular chemistry

How to cite: *Angew. Chem. Int. Ed.* **2015**, *54*, 4517–4521
Angew. Chem. **2015**, *127*, 4600–4604

[1] a) J. H. Wen, L. G. Vincent, A. Fuhrmann, Y. Choi, K. C. Hribar, H. Taylor-Weiner, S. Chen, A. J. Engler, *Nat. Mater.* **2014**, *10*, 979–987; b) F. Rossi, M. Santoro, G. Perale, *J. Tissue Eng. Regen. Med.* **2013**, DOI: 10.1002/term.1827; c) K. A. Kilian, M. Mrksich, *Angew. Chem. Int. Ed.* **2012**, *51*, 4891–4895; *Angew. Chem.* **2012**, *124*, 4975–4979.
[2] S. Gemini-Piperni, E. R. Takamori, S. C. Sartoretto, K. B. S. Paiva, J. M. Granjeiro, R. C. de Oliveira, W. F. Zambuzzi, *Arch. Biochem. Biophys.* **2014**, *561*, 88–98.
[3] J. Xiong, M. Onal, R. L. Jilka, R. S. Weinstein, S. C. Manolagas, C. A. O'Brien, *Nat. Med.* **2011**, *17*, 1235–1241.
[4] a) S. Shah, A. Solanki, P. K. Sasmal, K. B. Lee, *J. Am. Chem. Soc.* **2013**, *135*, 15682–15685; b) D. R. Griffin, A. M. Kasko, *J. Am. Chem. Soc.* **2012**, *134*, 13103–13107; c) M. He, J. Li, S. Tan, R. Wang, Y. Zhang, *J. Am. Chem. Soc.* **2013**, *135*, 18718–18721.
[5] B. P. Purcell, D. Lobb, M. B. Charati, S. M. Dorsey, R. J. Wade, K. N. Zellars, H. Doviak, S. Pettaway, C. B. Logdon, J. A. Shuman, P. D. Freels, J. H. Gorman III, R. C. Gorman, F. G. Spinale, J. A. Burdick, *Nat. Mater.* **2014**, *13*, 653–661.
[6] O. Z. Fisher, A. Khademhosseini, R. Langer, N. A. Peppas, *Acc. Chem. Res.* **2010**, *43*, 419–428.
[7] A. Banerjee, M. Arha, S. Choudhary, R. S. Ashton, S. R. Bhatia, D. V. Schaffer, R. S. Kane, *Biomaterials* **2009**, *30*, 4695–4699.
[8] J. Kim, Y. Park, G. Tae, K. B. Lee, C. M. Hwang, S. J. Hwang, I. S. Kim, I. Noh, K. Sun, *J. Biomed. Mater. Res. Part A* **2009**, *88*, 967–975.
[9] P. Bajaj, X. Tang, T. A. Saif, R. Bashir, *J. Biomed. Mater. Res. Part A* **2010**, *95*, 1261–1269.
[10] H. Mori, A. Takahashi, A. Horimoto, M. Hara, *Neurosci. Lett.* **2013**, *555*, 1–6.
[11] A. J. Engler, S. Sen, H. L. Sweeney, D. E. Discher, *Cell* **2006**, *126*, 677–689.
[12] A. S. Khalil, A. W. Xie, W. L. Murphy, *ACS Chem. Biol.* **2014**, *9*, 45–56.
[13] a) G. Godeau, C. Brun, H. Arnion, C. Staedel, P. Barthélémy, *Tetrahedron Lett.* **2010**, *51*, 1012–1015; b) S. Ziane, S. Schlaubitz, S. Miraux, A. Patwa, C. Lalande, L. Bilem, S. Lepreux, B. Rousseau, J.-F. Le Meins, L. Latxague, P. Barthélémy, O. Chassande, *eCM* **2012**, *23*, 147–160.
[14] a) L. A. Estroff, A. D. Hamilton, *Chem. Rev.* **2004**, *104*, 1201–1218; b) M. Brard, M. Richter, T. Benvegnu, D. Plusquellec, *J. Am. Chem. Soc.* **2004**, *126*, 10003–11012; c) A. Meister, A. Blume, *Curr. Opin. Colloid Interface Sci.* **2007**, *12*, 138–147; d) Y. Yan, T. Lu, J. Huang, *J. Colloid Interface Sci.* **2009**, *337*, 1–10; e) A. Meister, A. Blume, *Adv. Planar Lipid Bilayers* **2012**, *16*, 93–128; f) A. Blume, S. Drescher, G. Graf, K. Köhler, A. Meister, *Adv. Colloid Interface Sci.* **2014**, *208*, 264–278.
[15] J. H. Fuhrhop, T. Wang, *Chem. Rev.* **2004**, *104*, 2901–2937.
[16] a) J. Gaucheron, C. Santaella, P. Vierling, *Bioconjugate Chem.* **2001**, *12*, 569–575; b) M. Brunelle, A. Polidori, S. Denoyelle, A.-S. Fabiano, P. Y. Vuillaume, S. Laurent-Lewandowski, B. Pucci, *C. R. Chim.* **2009**, *12*, 188–208; c) N. Jain, V. Goldscmidt, S. Oncul, Y. Arntz, G. Duportail, Y. Mély, A. S. Klymchenko, *Int. J. Pharm.* **2012**, *423*, 392–400; d) N. Nuraje, H. Bai, K. Su, *Prog. Polym. Sci.* **2013**, *38*, 302–343.
[17] a) R. Iwaura, K. Yoshida, M. Masuda, K. Yase, T. Shimizu, *Chem. Mater.* **2002**, *14*, 3047–3053; b) R. Iwaura, K. Yoshida, M.

Masuda, M. Ohnishi-Kameyama, M. Yoshida, T. Shimizu, *Angew. Chem. Int. Ed.* **2003**, *42*, 1009 – 1012; *Angew. Chem.* **2003**, *115*, 1039 – 1042.

[18] a) G. Godeau, J. Bernard, C. Staedel, P. Barthélémy, *Chem. Commun.* **2009**, 5127 – 5129; b) L. Latxague, S. Ziane, O. Chassande, A. Patwa, M.-J. Dalila, P. Barthélémy, *Chem. Commun.* **2011**, *47*, 12598 – 12600.

[19] T. A. Ulrich, A. Jain, K. Tanner, J. L. MacKay, S. Kumar, *Biomaterials* **2010**, *31*, 1875 – 1884.

[20] a) B. Xing, C.-W. Yu, K.-H. Chow, P.-L. Ho, D. Fu, N. Xu, *J. Am. Chem. Soc.* **2002**, *124*, 14846 – 14847; b) P. Terech, R. G. Weiss, *Chem. Rev.* **1997**, *97*, 3133 – 3159; c) S. Banerjee, R. K. Das, U. Maitra, *J. Mater. Chem.* **2009**, *19*, 6649 – 6687; d) D. J. Abdallah, R. G. Weiss, *Adv. Mater.* **2000**, *12*, 1237 – 1247.

[21] M. J. Clemente, P. Romero, J. L. Serrano, J. Fitremann, L. Oriol, *Chem. Mater.* **2012**, *24*, 3847 – 3858.

[22] a) B. D. Olsen, J. A. Kornfield, D. A. Tirrell, *Macromolecules* **2010**, *43*, 9094 – 9099; b) W. Wang, L. Deng, S. Xu, X. Zhao, N. Lv, G. Zhang, N. Gu, R. Hu, J. Zhang, J. Liu, A. Dong, *J. Mater. Chem. B* **2013**, *1*, 552 – 563; c) A. Baral, S. Roy, A. Dehsorkhi, I. W. Hamley, S. Mohapatra, S. Ghosh, A. Banerjee, *Langmuir* **2014**, *30*, 929 – 936; d) J. Nanda, A. Biswas, A. Banerjee, *Soft Matter* **2013**, *9*, 4198 – 4208.

[23] B. J. Lawrence, S. V. Madihally, *Adhes. Migr.* **2008**, *2*, 9 – 16.

Received: September 15, 2014
Revised: November 5, 2014
Published online: February 18, 2015

